Mev information, are presented in Table II. They have been calculated in the same way as were the values for $E_n=220$, except that the effects of finite pulse-height resolution and angular resolution have been neglected. This is justified when the pulse-height spectra do not change slope rapidly compared with the resolution widths. These values of $\sigma(\theta)$ for 180 Mev are plotted in Fig. 6, in which the solid curve is the same as was used for integration of the 220-Mev data but normalized to a total cross section of 44 mb.[2] The value of K taken for these data was 0.144, which fitted the points to the normalizing curve more or less closely. This distribution exhibits the expected gross features, but details of shape, unfortunately, are not significant.

The authors wish to express their appreciation to Professsor A. Roberts for his interest in this problem and his generous assistance with the performance and analysis of the experiment.

PHYSICAL REVIEW VOLUME 88, NUMBER 1 OCTOBER 1, 1952

Excitation Functions to 100 Mev*

NORTON M. HINTZ† AND NORMAN F. RAMSEY
Nuclear Laboratory, Harvard University, Cambridge, Massachusetts
(Received June 2, 1952)

A method is described for obtaining excitation functions using the stacked foil technique with an internal cyclotron beam. The method, which utilizes multiple Coulomb scattering for deflection and 180° focusing for energy separation, has the advantages of good energy resolution, high intensity, and low background. Equations are presented for the particle orbits from which are derived the energy resolution and efficiency attainable. Absolute excitation curves are given for the reactions, $C^{12}(p,pn)C^{11}$; Na^{24}, Na^{22}, and F^{18} from Al^{27}; $B^{11}(p,n)C^{11}$; and $S^{34}(p,n)Cl^{34}$. Absolute cross sections are determined using the monitor reaction, $C^{12}(p,pn)C^{11}$, and the ratio of the β-counting rates. Various corrections to the relative and absolute excitation curves are discussed. A brief interpretation of the results is given in which it is argued that they are consistent with present ideas about high energy nuclear reactions.

1. INTRODUCTION

THE sparsity of data on excitation functions of nuclear reactions above 30 Mev made it worthwhile to begin a systematic study in this field with the 100-Mev protons from the Harvard cyclotron. Some of the results of this investigation have already been published[1–3] together with a brief account of the method used. It is the purpose of this paper to describe the method more fully and to present some additional excitation curves.

At energies of a few tens of Mev one expects individual variations in nuclear structure to have little effect on the excitation curves, the main features of which should depend on the more general properties of nuclei such as the average nucleon density, the momentum distribution of the nucleons, the mean free path of fast nucleons in nuclear matter, and the average level density at large excitation. Accordingly, it was felt that a method should be devised by means of which a few reactions could be done with reasonably high accuracy, especially those which were of particular use in monitoring high energy proton flux, and by means of which the main features of a large number of other reactions could be obtained quickly and with economy of cyclotron time.

The classical method of stacked foils[4] satisfies these requirements well at low energies where no special difficulties are met with in beam deflection, extraction, and intensity. However, at 100 Mev, the present techniques of extraction are highly inefficient and therefore lead to serious problems of intensity or energy resolution. To overcome these difficulties it was decided to use the stacked foil method with the internal cyclotron beam, making use of the focusing properties of the uniform magnetic field to provide a nearly monochromatic beam of reasonable intensity. A somewhat similar technique has been used by Chupp and McMillan[5] with the protons stripped from fast deuterons. However, due to the broad energy distribution of their protons, the choice of carbon as an absorber, and the high neutron background their results were inaccurate.

2. EXPERIMENTAL GEOMETRY AND PARTICLE ORBITS

The method of stacked foils is unsatisfactory for use directly with the circulating beam of a frequency modulated cyclotron for two reasons. First, the small gain in orbit radius per turn (~1 mil) makes it impossible to align the foil and absorber assembly in such a way that all targets receive the same proton flux.

* Assisted by the joint program of the ONR and AEC.
† Present address: Department of Physics, University of Minnesota, Minneapolis, Minnesota.
[1] Norton M. Hintz, Phys. Rev. **83**, 185 (1951).
[2] J. W. Meadows and R. B. Holt, Phys. Rev. **83**, 47 (1951).
[3] J. W. Meadows and R. B. Holt, Phys. Rev. **83**, 1257 (1951).
[4] E. O. Lawrence, Phys. Rev. **47**, 17 (1935).
[5] W. W. Chupp and E. M. McMillan, Phys. Rev. **72**, 873 (1947).

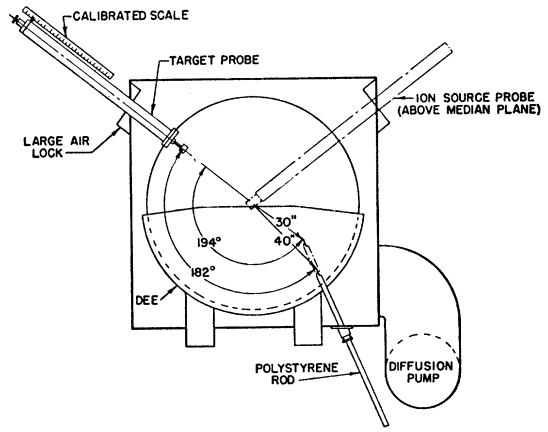

FIG. 1. Geometry of scattering and target probes in "180°" arrangement.

Second, the energy spread of the primary beam, which is probably due to radial oscillations, results in very poor energy resolution, especially for foils well down in the absorber stack. This is because an initial energy spread, ΔE_0, increases approximately as $1/E$ as the particles penetrate the absorbers, due to the $1/E$ dependence of the stopping cross section. Since the range spread, ΔR_0, corresponding to ΔE_0, remains constant as the particles pass through the absorber, the fractional energy width $\Delta E/E$ is approximately,

$$\Delta E/E=(\Delta R_0/E)(dE/dR)_E\simeq(\Delta E_0/E_0)(E_0/E)^2, \quad (1)$$

and so increases very rapidly down the absorber stack. A 100-Mev proton beam must be monochromatic to better than 1 percent initially if the energy resolution is to be limited by ordinary range straggling.

Both of these difficulties can be overcome. f the protons are first deflected by multiple Coulomb scattering in a thin foil placed in the median plane. The stack of absorbers and targets can then be placed above or below the median plane of the cyclotron beam at an angular position, relative to the scatterer, which results in particles from a narrow momentum interval being focused on the target face. The actual geometry used is shown in Fig. 1. The target and absorber assembly is inserted on a calibrated radial probe which passes through a large vacuum lock. The assembly is held above or below the median plane a distance which is determined by two factors. The maximum amplitude of the vertical oscillations sets a lower limit and the aperture of the dee system an upper limit. Since the circulating beam must expand to a radius somewhat greater than that of the targets, it is essential that no protons strike the absorber assembly as they pass by it on their way to the scatterer. This would result in protons of lower energy than that defined by the scatter reaching the targets. For the Harvard cyclotron, virtually all of the protons have vertical oscillations less than $\frac{3}{4}$ in. at a radius of 30 in. At this same radius the dee aperture is $\pm 1\frac{3}{4}$ in. Thus the target assembly could lie between about $\frac{7}{8}$ in. and $1\frac{5}{8}$ in., allowing a small margin for error in placement. This fixes the maximum foil diameter and hence the maximum efficiency attainable.

The scatterer consists of a strip of tantalum foil, of approximately the thickness for maximum scattering efficiency ($\sim$5 mils), fixed to the end of a polystyrene rod which passes through an existing hole in the cyclotron dee. This hole, which almost completely determined the scatterer position, was fortunately located very near the correct angle for energy focusing.

The equations which describe the proton orbits before and after scattering will be given briefly for their use in determining the target and scatterer positions, the scatterer thickness, and the expected energy resolution and efficiency.

If the magnetic field is nearly uniform,

$$[n=(r/H)\partial H/\partial r\ll 1],$$

the proton orbits may be taken as circles upon which are superposed small periodic radial and vertical displacements[6] of frequencies ω_r and ω_v and amplitudes A_r and A_v. These frequencies are given by

$$\omega_r=\omega_0(1-n)^{\frac{1}{2}}, \quad \omega_v=\omega_0(n)^{\frac{1}{2}}, \quad (2)$$

where ω_0 is the orbital frequency. If A_r and A_v are small relative to r, we may discuss the radial and vertical motions independently.

We first consider the particle orbits projected in the median plane. The orbital angle, θ_0, is to be measured from the scatterer position; the radial co-ordinate, r, from the cyclotron center. Just before scattering the orbit may be described by

$$r=r_0+A_r\cos(\theta_r+\delta_r), \quad (3)$$

where $\theta_r=\omega_r t=\theta_0(1-n)^{\frac{1}{2}}$ and r_0 is the radius of a particle of the same energy in a stable orbit. The phase factor, δ_r, is small since all particles will be nearly at the maximum in their radial oscillation when intercepted by the scatterer as a consequence of the small gain in orbit radius per revolution. A calculation shows $\delta_r\simeq 10^{-2}$ radian as a maximum value. When a proton passes through the scatterer its direction will change and it will lose energy. The change in direction corresponds to an additional radial oscillation of phase zero and amplitude, A_s, which is to be superposed on that already present. The energy loss will correspond to a sudden decrease in the stable orbit radius by an amount Δr_0, but since the radial coordinate of the particle does not change, an additional radial oscillation of amplitude Δr_0 and phase $\pi/2$ must be superposed. Thus, after scattering, the orbit may be written

$$r=r_0+\Delta r_0(\cos\theta_r-1)+A_r\cos(\theta_r+\delta_r)+A_s\sin\theta_r. \quad (4)$$

The scattering induced radial oscillation amplitude, A_s, will be related to the projected scattering angle,

[6] D. W. Kerst and R. Serber, Phys. Rev. **60**, 53 (1941).

α_r, by

$$\alpha_r=\left[\left(\frac{dr}{d\theta_0}\right)_f-\left(\frac{dr}{d\theta_0}\right)_i\right]\Big/r,$$

evaluated at $\theta_0=0$. The subscripts i and f indicate the derivative before and after scattering. This gives

$$A_s=r_s\alpha_r(1-n)^{-\frac{1}{2}}, \tag{5}$$

where r_s, the scatterer radius, is written

$$r_s=r_0+A_r\cos\delta_r.$$

At $\theta_r=2\pi$, or $\theta_0=2\pi(1-n)^{-\frac{1}{2}}$, $r=r_s$ from Eq. (4) and particles of all energy are refocused at the scatterer radius. This is the proper target position for maximum intensity and minimum energy resolution. In practice, the targets may be placed directly above or below the scatterer when maximum intensity is desired since $(1-n)^{-\frac{1}{2}}\simeq 1$ and the scattered beam will be refocused to within the target width at $\theta_0=2\pi$.

At $\theta_r=\pi$, or $\theta_0=\pi(1-n)^{-\frac{1}{2}}$, Eq. (4) gives $r=2(r_0-\Delta r_0)-r_s$, which is the same for all particles of the same energy independent of A_r, α_r, and δ_r. This is the well-known result for "180°" focusing, to first order, of particles from a line source in a uniform magnetic field. The innermost edge of the scatterer corresponds to the line source.

The over-all efficiency of the "180°" and "360°" arrangements will be determined by the motion of the particles in the vertical direction and, in the case of "180°" focusing, by the energy spectrum of the primary circulating beam. By analogy with the above, the motion in the Z direction, perpendicular to the median plane, will be given by

$$Z=A_v\sin(\theta_v+\delta_v)+A_s'\sin\theta_v \tag{6}$$

after scattering. A_s' is the scattering induced vertical oscillation given by

$$A_s'=r_s\alpha_v n^{-\frac{1}{2}} \tag{7}$$

where α_v is the projected vertical scattering deflection. Here δ_v will not in general be small since the particles will strike the scatterer at all phases in their vertical oscillation.

The distribution in α_r and α_v will be approximately Gaussian,[7] with

$$\langle\alpha_r^2\rangle_{Av}=\langle\alpha_v^2\rangle_{Av}=\langle\alpha^2\rangle_{Av}=B\log(\theta_2/\theta_1). \tag{8}$$

θ_1, θ_2, and B are defined in the reference. If the innermost edge of the scatterer is aligned vertically, the δ_v will be distributed randomly, and the mean square value of Z after scattering and at an angle θ_0 will be

$$\langle Z^2\rangle_{Av}=\tfrac{1}{2}\langle A_v^2\rangle_{Av}+r_s^2n^{-1}\langle\alpha_v^2\rangle_{Av}\sin^2(\theta_0n^{\frac{1}{2}}). \tag{9}$$

If the distribution in A_v can be taken as approximately Gaussian, the fraction of the particles which are scattered into the angular range defined by the vertical dimension of the target will be, for a single traversal of the scatterer,

$$I=(2\pi\langle Z^2\rangle_{Av})^{-\frac{1}{2}}\int_{Z_1}^{Z_2}\exp[Z^2/2\langle Z^2\rangle_{Av}]dZ. \tag{10}$$

Z_1 and Z_2 are the coordinates of the vertical extremes of the target. I will be a maximum, for a given Z_1 and Z_2, if the scatterer thickness is chosen so that $\langle Z^2\rangle_{Av}^{\frac{1}{2}}$, as calculated from Eq. (9), is equal to $\frac{1}{2}(Z_1+Z_2)$, i.e., a particle which is scattered through the rms scattering angle should just be able to enter the target center. Actually, I is a rather slowly varying function of $\langle Z^2\rangle_{Av}$ so a single scatterer can be used over a fairly wide energy range. A scatterer of high nuclear charge should be used to minimize the energy loss for a given rms scattering angle.

Not all particles which are scattered into the range defined by Z_1 and Z_2 will enter the targets since they must have the correct radial coordinate as well. In the "360°" case ($\theta_0=2\pi(1-n)^{-\frac{1}{2}}$) all particles will have the correct radius and the efficiency of the arrangement as calculated from Eq. (10) will be about 7 percent for $\frac{5}{16}$-in. diameter targets placed with their center one inch from the median plane. For the "180°" case the efficiency is roughly 0.7 percent, as determined by Eq. (10) and the fraction of all particles which lie within the energy range subtended by the targets. The intensity available with this method, even with the rather broad energy spectrum of the Harvard cyclotron, is of the order of 10^{-9} amp/cm^2 which is considerably greater than that which can be obtained in an external magnetically analyzed beam.

As stated previously, the targets could not be placed exactly at the correct angles for "180°" focusing because of cyclotron geometry. However, due to the small angular aperture of the Coulomb scattered beam, the focusing error was never greater than the target width. In the "180°" case, if β is the angle by which the actual geometry differs from $\pi(1-n)^{-\frac{1}{2}}$, the focusing error, Δf, is from Eq. (4):

$$\Delta f=\tfrac{1}{2}\beta^2(\Delta r_0+A_r)-\beta A_s. \tag{11}$$

Δf is defined as the radial width, at the target position, of a group of scattered particles of the same energy. For $\beta=10°$, the maximum deviation used, the rms value of Δf is about 0.1 in., which is roughly equal to the half-width of the targets when $\frac{5}{16}$-in. diameter foils are used. Thus the energy resolution is determined primarily by the target width and range straggling. A small contribution to the energy width at the targets can come from a finite source width due to penetration of the primary particles back from the innermost edge of the scatterer.[8,9] A radioautograph of the scatterer showed ~90 percent of the activity to be concentrated

[7] E. J. Williams, Proc. Roy. Soc. (London) **169**, 531 (1939).

[8] W. J. Knox, Phys. Rev. **81**, 693 (1951).

[9] Cassels, Dickensen, and Howlett, Proc. Phys. Soc. **B64**, 590 (1951).

within 1 mm of the edge. An experiment to measure the energy distribution of the scattered beam is discussed in Appendix A.

3. TARGET ASSEMBLY AND BOMBARDMENT PROCEDURE

The choice of an absorber material to degrade the proton energy was based on the following considerations. For a given energy loss in the absorbers it is desired to (1) minimize loss of particles due to multiple scattering, (2) minimize nuclear interactions in the absorbers which would give neutron and proton secondaries and decrease the incident proton flux. To satisfy requirement (1) the mean square displacement, after traversing a given energy range, should be minimized. This is best done using elements of low nuclear charge and high density, the latter being more important. In this respect, copper and uranium are about equally good and about twice as good as aluminum or carbon. In respect to (2), one gains steadily by going to heavier elements but only as $A^{\frac{1}{3}}$, so factor (1) is more important. Considering availability and machinability, brass is an excellent choice. Fortunately the relative stopping power of zinc to copper is unity to within one part in one thousand over the crucial energy range, so the computed range-energy curves for copper could be used. A relatively heavy element is also desired in order to minimize contamination of the targets due to nuclear recoils from the absorbers. Occasionally thin aluminum absorbers were used for small energy steps but only over a small range interval so that losses due to multiple scattering were small. Since the dispersion in energy, due to range-straggling, is approximately independent of the substance for a given energy loss this factor does not enter into the choice of the absorber material.

The absorber-target geometry should be such that all foils should receive the same proton flux and all protons which can activate the foils should pass through the same absorber thickness. This is usually done by placing the foils and absorbers behind a collimating hole of smaller diameter. However, it was found that any material in front of the targets spoiled the energy resolution and increased the neutron background. Consequently, the absorbers were made $\frac{1}{16}$ in. larger in diameter than the foils and no collimation used. Each absorber was recessed slightly to take the target foil or pellet and a cap, with a raised center portion, was fitted so that the total absorber thickness was the same everywhere. By having the absorbers slightly larger than the foils, protons scattered out of the foil area are partly compensated for by protons scattered in from the surrounding absorber area. This will be discussed in Appendix B.

The absorber density was determined by a volumetric and a gravimetric method, the two results checking to within 0.3 percent. The foils were punched with a precision ground dowel pin fitting into a jig bushing. Pellets were pressed with a similar arrangement. The foils or pellets were weighed, usually after counting, on a microbalance to ± 0.02 mg. For irradiation, the stack of absorbers and targets was fitted into a brass capsule. This was then held at a suitable distance from the median plane on a radial probe (Fig. 1, reference 1). Altogether the foils were then surrounded by $\frac{3}{16}$ in. of brass giving shielding against low energy protons entering the stack sideways. The background due to such protons was then found to be less than 0.1 percent.

Several such targets can be irradiated simultaneously above and below the median plane when more efficient use of cyclotron time is desired. Since the width of the radial oscillation distribution is about 2.5 in. for the Harvard cyclotron, the radial half-width of the scattered beam at $\theta_0=\pi(1-n)^{-\frac{1}{2}}$ is 5 in., allowing room for several targets at slightly different radii.

When the yield of one reaction was being used to calibrate the cross section for another, the irradiation time was kept short relative to the shorter of the two half-lives and the cyclotron was given a preliminary warm-up to ensure steadiness during the run. Zero time was taken at the midpoint of the bombarding interval.

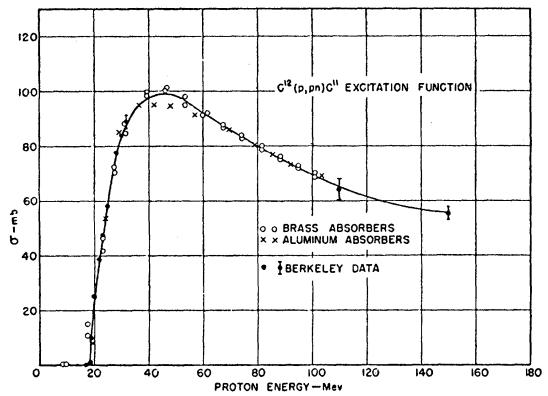

FIG. 2. Data for $C^{12}(p,pn)C^{11}$ reaction normalized to Berkeley data (Aamodt *et al.*, reference 9) at 32 Mev.

4. RELATIVE EXCITATION FUNCTIONS

After irradiation the samples were counted in well-defined geometry in a shielded sample changer containing a thin mica end-window Geiger tube. The short and long term stability of the counter was checked from time to time with a standard source and found to be within the statistical limits if the Geiger tube was left continuously at the operating voltage.

The raw counter data was corrected for counter background, dead time losses, decay since zero time, and neutron induced activity. The latter was evidenced by activity in foils placed beyond the proton range and was usually of the order of 2 percent.

After these corrections, two further ones must be considered before the corrected counting rates for a given activity can be taken as a relative excitation function. These are, the losses of protons from the foil

area caused by nuclear collisions and by Coulomb scattering. As will be discussed in Appendix B, the latter can be made negligible by surrounding the foils with material whose thickness is several times larger than the rms displacement of protons which traverse the absorber stack. The loss of protons due to nuclear effects is difficult to determine since the second foil of the stack is in "very poor" geometry relative to the first while the last is intermediate between "poor" and "good" geometry. Somewhat arbitrarily the data have been corrected using $\sigma_a=\pi R^2$ as the nuclear absorption cross section. A value of $R=1.4\times10^{-13}A^{\frac{1}{3}}$ has been chosen. This should over correct for the first few foils and undercorrect for the last few. Since the maximum correction for nuclear absorption was about 10 percent, the overall uncertainty in the relative cross section should be not more than $\sim$3 percent. Some evidence to support this comes from the fit obtained to the absolute cross sections measured at 32 Mev and 110 Mev[10] when our data are so corrected. This is shown in Fig. 2.

The energy of the protons at each target foil was calculated from the average radius and magnetic field for the scattered protons together with range-energy curves calculated from the Bethe-Bloch formula.[11] Allowance was made for the stopping effect of the target foils or pellets. The magnetic field was measured by U. E. Kruse and G. Watkins to within 0.01 percent using a nuclear resonance method.

5. ABSOLUTE CROSS SECTIONS

Because of effects resulting from rf pick-up and neutron background, a direct measurement of the proton current to the targets, from inside of the cyclotron vacuum system, was not feasible and it was decided to use the $C^{12}(p,pn)C^{11}$ reaction in order to monitor the proton current. By normalizing the relative excitation function for C^{11}, obtained as described here, to the absolute values at 32 and 110 Mev of Aamodt *et al.*,[10] a curve resulted which gave the absolute cross section in the region from the threshold to 100 Mev to within 5–10 percent.

The monitor foils of polyethylene or polystyrene were the same diameter, $\frac{5}{16}$ in. or $\frac{7}{16}$ in., as the target foils and from 3 to 5 mils in thickness. They were placed either in contact with or in separate absorbers from the target foils. If the monitor foil is placed near the target foil, so that both receive the same proton flux, the cross section for a reaction, Z, in terms of the monitor reaction, M, is:

$$\sigma_Z=\sigma_M R_Z n_M \tau_Z / R_M n_Z \tau_M, \qquad (12)$$

where R is the disintegration rate extrapolated to zero time, n the number of target nuclei per cm^2 and τ the half-life. It is assumed that the irradiation time is short as compared with the τ's.

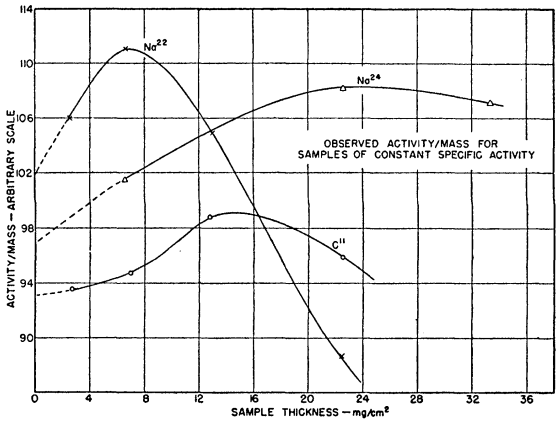

FIG. 3. Curves to determine correction for self absorption and scattering in β-ray samples.

The ratio R_Z/R_M was determined by counting the β-activity of the residual nuclei. The target and monitor foils were mounted on Lucite or copper planchets, of sufficient thickness to ensure saturation backscattering,[12] and counted in identical geometry with the same Geiger tube. The general procedure for applying corrections to the observed counting rates for absorption and scattering have been discussed by several authors[12–14] and will be mentioned only briefly. The correction for absorption of the β-rays in the air and window of the counter was made from an absorption curve taken on a thin source (5–10 mg/cm^2) with the absorbers placed against the counter window to insure linearity. The scattering effect of the air between sample and window has been found to be less than 1 percent for the geometry used in this experiment.[12] The correction for absorption and scattering of the β-rays in the sample itself is determined by extrapolating to zero sample thickness a curve of counting rate *vs* sample thickness for samples of constant specific activity. Such samples are produced by irradiating targets of various thicknesses at the same position in the absorber stack. Resultant curves for several activities are shown in Fig. 3. The increase of counting rate due to back-scattering has been found to be independent of β-ray energy for β-distributions of maximum energy greater than 0.3 Mev provided the sample backing is of sufficient thickness to give saturation backscattering.[13] However, some recent work[15] has shown a possible difference in the saturation backscattering of electrons and positrons which, if it exists, would give an error of $\sim+10$ percent in the absolute values for the Na^{24} cross section. The aluminum counter

[10] Aamodt, Peterson, and Phillips, unpublished University of California Radiation Laboratory Report No. 1400.
[11] Aron, Hoffman, and Williams, unpublished University of California Radiation Laboratory Report No. 121.
[12] L. R. Zumwalt, unpublished Atomic Energy Commission Unclassified Report No. 567.
[13] B. P. Burtt, Nucleonics 5, 28 (1949).
[14] Conference on Absolute β-Counting, unpublished Report No. 8, National Research Council (1950).
[15] H. H. Seliger, J. Research Natl. Bur. Standards 47, 41 (1951).

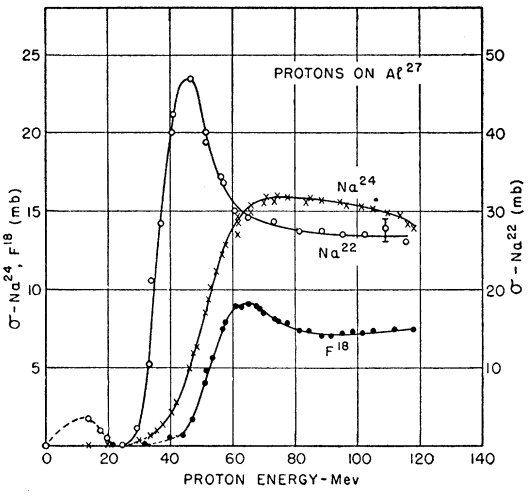

FIG. 4. Multiple particle reactions from protons on Al^{27}. Note ordinate scale at right for Na^{22} yield.

housing has been found to have a negligible effect on the counting rates if the samples are close to the window.[14]

If the corrections mentioned above are made on the observed counting rates, the counter efficiency has been shown to be independent of β-ray energy from 0.3 to 2.3 Mev maximum.[12] The over-all accuracy of this procedure is certainly not better than 10 percent for β-rays above 1 Mev and probably 20 percent for those of lower energy.

As an independent check on the value of the cross section for the reaction $Al^{27}(p,3pn)Na^{24}$ obtained from the corrected β-ray count, a direct β-γ coincidence calibration was made of the ratio $R(Na^{24})/R(C^{11})$. In the case of C^{11}, which emits no γ-rays, the positrons were counted in coincidence with the annihilation radiation.[16] The Na^{24} source was coincidence-calibrated in the usual way. When corrections of a few percent were made for the γ-sensitivity of the β-crystal, the ratio $R(Na^{24})/R(C^{11})$ agreed to within 3 percent with that determined as described above. This result does not imply the same reliability for the other absolute cross sections, since in general the corrections for absorption and scattering of the β-rays were greater than in the case of the Na^{24}/C^{11} ratio. However, it seems to rule out the possibility of gross errors in the extrapolations involved in determining these absorption corrections.

6. RESULTS

A. $C^{12}(p,pn)C^{11}$

The final data for this reaction is shown in Fig. 2. Bombardments of one or two minutes were sufficient to give 1 percent statistics in a one minute counting interval with 0.005-in. polystyrene foils so that as many as twenty foils could be run in the stack. The smooth fit of our data to the results of Aamodt *et al.*[10] at 110 Mev and 32 Mev gives good evidence for the over-all reliability of the method and provides a check on our absolute energy scale and resolution. A shift of 1 Mev at the bombarding energy of 100 Mev would give a noticeable discrepancy with the linear accelerator data at the threshold.

B. Na^{24}, Na^{22}, and F^{18} from Al^{27}

These nuclei were identified by their half-lives, absorption characteristics and chemistry and were easily resolved from the decay curves without chemical separation. Considerable 10 and 20-minute activity was also present in the aluminum foils, presumably due to fission reactions leading to C^{11} and N^{13}, but this could not be resolved. To determine the absolute cross sections, polyethylene monitor foils were included in the target assembly. A bombardment of 4–6 min gave sufficient activity to obtain the ratios $\sigma(C^{11})/\sigma(Na^{24})$ and $\sigma(C^{11})/\sigma(F^{18})$. The Na^{24} yield was then used as a secondary monitor in the longer runs of several hours needed to give sufficient Na^{22} intensity. The absolute excitation functions for these reactions are shown in Fig. 4 where the combined results of several runs for each curve are plotted. The rise of the Na^{22} curve below 20 Mev is probably a contamination effect since it occurs at a rather low energy for even a (p,Li^6) reaction. There is some evidence[17] for K-capture in the decay of F^{18} which, if it exists, would raise the value of $\sigma(F^{18})$ shown in Fig. 4. Some doubt has arisen as to the correctness of the Na^{22} absolute cross section. J. B. Harding[18] has determined the ratio $\sigma(Na^{22})/\sigma(Na^{24})$ by counting the γ-radiation in both cases with a calibrated scintillation crystal. He obtains a value of about half of ours. The cause of this discrepancy is not known.

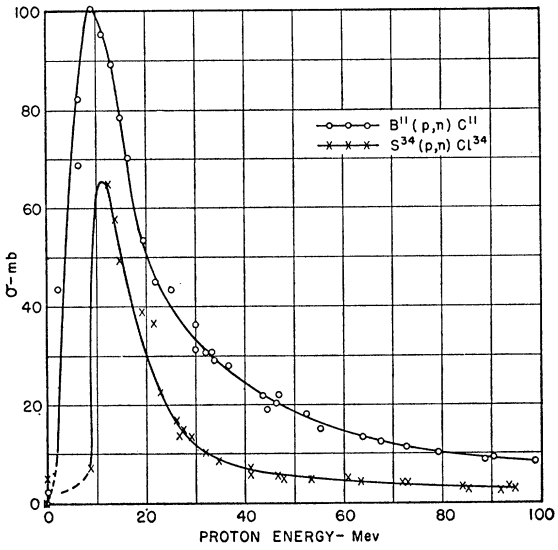

FIG. 5. Excitation functions for two (p,n) reactions.

[16] Birge, Kruse, and Ramsey, Phys. Rev. **83**, 274 (1951).

[17] Z. W. Ho, Compt. rend. **226**, 1187 (1948).

[18] A. E. R. E. Harwell (private communication).

C. $B^{11}(p,n)C^{11}$ and $S^{34}(p,n)Cl^{34}$

After the rather complicated reactions on aluminum, it was thought worthwhile to look at a simple reaction, (p,n), for several nuclei. The results of the first two such reactions are shown in Fig. 5. Even simpler reactions of the type $X(p,p')X^*$ could be studied by the activation technique using such stable nuclei as Sr^{81}, Rh^{103}, In^{115}, etc., which have isomeric states.

Powdered natural boron (81 percent B^{11}) was used for the $B^{11}(p,n)C^{11}$ reaction. The C^{11} yield from the 19 percent of B^{10} by a (p,γ) reaction should be negligible except below the (p,n) threshold. The powdered boron could not be pressed into pellets, so recessed absorbers with tight fitting caps were used to hold the powder. Two runs were made at 100 Mev to obtain the main features of the excitation curve above 30 Mev. After this, numerous runs were made at an incident energy of 60 Mev, shifting the energy scale slightly at each run by adding a thin absorber to obtain detail in the low energy peak. Each run was separately monitored with the C^{11} reaction, and all points reduced to absolute cross sections for plotting. The absolute cross sections, in terms of that of C^{11}, should be quite accurate since in both cases the same activity was being counted and the samples were adjusted to have the same thickness. The points below 10 Mev are badly smeared because of straggling and should not be taken seriously. The activity of boron samples beyond the proton range was less than 0.05 percent of the peak. This is evidence for the very small background of protons which might have entered the absorber stack from the side.

The reaction $S^{34}(p,n)Cl^{34}$ leads to an energetic (3–5 Mev) β-emitter with a 32-min period whose decay scheme is not well known.[19] Natural sulfur (4.2 percent S^{34}) was used although isotopic enrichment would have improved the accuracy. The interfering activities (P^{32}, Si^{31}) were eliminated by counting the samples through a thick absorber. If a small 15-hour background was subtracted the samples decayed from about 50 min to 4 hours with a slope of 32 ± 0.5 min. This half-life was checked against a purified Cl^{34} source obtained by irradiating Na_2SO_4 and precipitating AgCl. This gave a period of 32.5 ± 0.5 min over 10 half-lives. The absolute values shown in Fig. 5 are rather approximate (±25 percent) since thick samples and absorbers were used, resulting in rather large corrections to the β-count. In calculating $\sigma(Cl^{34})$, one β-ray per disintegration was assumed.

An excitation curve for Cu^{62} (10.2 min, β^+) from natural copper is shown in Fig. 6. This was taken as a preliminary to work in progress on the separated isotopes. The large peak at 25 Mev is the result of the $Cu^{63}(p,pn)Cu^{62}$ reaction while the smaller peak at 50 Mev is probably the $Cu^{65}(p,p3n)Cu^{62}$ reaction.

[19] L. Ruby and J. R. Richardson, Phys. Rev. **83**, 698 (1951).

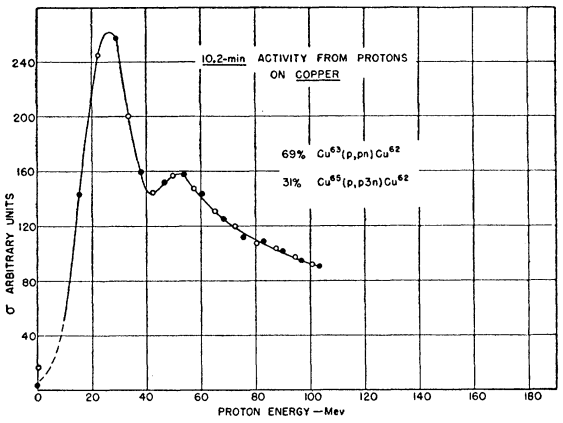

FIG. 6. Cu^{62} from natural copper.

7. ERRORS

A possible error in both the relative and absolute cross sections is the loss of nuclei from the target foils due to recoil or evaporation during bombardment. The first of these has been discussed in another paper in connection with its use to determine the momentum transfer in high energy nuclear reactions.[20] For the C^{11} and Na^{24} reactions the loss is about 5–10 percent for 1-mil foils. Since 5-mil foils were generally used, the recoil loss is less than the uncertainty in the proton absorption correction, and further, tends to cancel in the ratio R_Z/R_M. This will also be true for the F^{18} and Na^{22} reactions. The recoil losses for the two (p,n) reactions should be even less since a smaller momentum transfer to the residual nucleus is expected. There will in these cases be an error of a few percent in the absolute cross sections due to recoil losses from the monitor foil.

The loss of product nuclei by evaporation from the targets during irradiation has been reported to be small if the targets are not overheated.[21,22] An experiment was performed to measure the F^{18} and Cl^{34} yield when the targets were held at atmospheric pressure in a vacuum-tight capsule during irradiation. The values obtained were 10 percent high for F^{18} and 15 percent high for Cl^{34} as compared to the average values from several runs in which vacuum-tight capsules were not used. Although these corrections are within the errors in the absolute ratio of the β-counts they have been included in the curves presented. Other sources of error in the relative excitation curves would be the finite energy width of the scattered beam and the subsequent straggling in the absorber as well as any errors in the absolute energy scale. The spectrum of the "180°" scattered protons was measured at the target position. The method and results are given in Appendix A. Protons initially monochromatic at 100 Mev will have a dispersion of 4 Mev at 20 Mev, which will lower the peaks in the (p,n) reactions by ~15

[20] N. M. Hintz, Phys. Rev. **86**, 1042 (1952).
[21] Brown, Irvine, and Livingston, J. Chem. Phys. **12**, 132 (1944).
[22] J. D. Seagrave, Phys. Rev. **84**, 1219 (1951).

TABLE I. Thresholds for Al^{27} reactions in laboratory system calculated from mass differences ($-Q$) and mass differences plus total Coulomb barrier heights ($-Q+V_B$).

Mode of decay	$-Q$, Mev	$-Q+V_B$, Mev
$Al^{27}(p,3pn)Na^{24}$	32	44
(p,pHe^3)	24	36
$Al^{27}(p,3p3n)Na^{22}$	52	64
$(p,T\ He^3)$	35	47
$(p,\alpha d)$	20	32
(p,Li^6)	18.5	30
$Al^{27}(p,5p5n)F^{18}$	91	110
$(p,\alpha T\ He^3)$	45	54
$(p,2\alpha d)$	30	49
(p,B^{10})	24	41

percent but will have little effect on the reactions with higher thresholds.

In summary, it is believed the relative values at different energies are correct to within ±5 percent, except in the case of the (p,n) peaks, the principal uncertainty being in the proton absorption correction. The absolute values should be within ±15 percent for Na^{24} and for C^{11} from B^{11} and ±25 percent for F^{18}, Na^{22}, and Cl^{34}, the uncertainty being in the absorption and scattering corrections to the β-ray count.

8. CONCLUSIONS

The reaction $C^{12}(p,pn)C^{11}$ has been discussed theoretically by Heckrotte and Wolff[23] using the evaporation theory at low energy and a rough independent particle model at higher energy. They predict a peak at 45 Mev to be followed by a slowly varying cross section up to 140 Mev where their calculations terminate. The peak found here is in fair agreement with their calculation. The earlier curve of Chupp and McMillan[15] did not show this peak due to the poorer energy resolution and higher neutron background. The slowly decreasing cross section above 45 Mev does not agree with the calculations of Heckrotte and Wolff, who predict a cross section which rises slowly above the peak and which has about half the value observed. The reason for the discrepancy is not clear from their brief account of the calculation. In any independent particle model the cross section must ultimately decrease approximately as $1/E$. The contribution to the C^{11} yield from a (p,d) reaction[24] would give a decreasing term of about 25 mb at 90 Mev.

The detailed interpretation of the reactions on Al^{27} along the lines of the C^{11} calculation would be quite difficult because of the many ways in which the reaction may proceed. In addition to the evaporation and fast knock-on neutrons and protons there is an appreciable contribution from the emission of α-particles, or other compound nuclei, as can be seen from an inspection of Table I in which the reaction thresholds for various modes of decay have been calculated. From Fig. 4 it seems likely that Na^{24} is produced mostly by a $(p,3pn)$ reaction although there is some evidence at the threshold for a (p,pHe^3) reaction. Na^{22} must definitely result in part from reactions of the kind $(p,\alpha pn)$ or (p,Li^6). Similarly, F^{18} cannot be made by a $(p,5p5n)$ process below 91 Mev, even allowing for barrier penetration. The slowly varying yield at high energy in these curves may then be due to an increasing contribution from processes in which the nucleons leave as individuals, superimposed on a decreasing tail from the evaporation of heavier fragments from a compound nucleus. This effect can be seen in a striking way in Fig. 1, reference 3, in which the (p,α) contribution to the production of Na^{22} from Mg^{25} has reached a very small value before the threshold of the $(p,2p2n)$ reaction occurs. A high probability for the evaporation of α-particles and other light fragments follows directly from phase-space and level density arguments alone[25] if these units are thought of as having at least a transient existence in the nucleus. In addition, because of increasing non-capture excitation at high energies as predicted by Serber[26] and verified by nuclear recoil measurements,[20] there is a tendency for the actual excitation of the nucleus to vary more slowly than the energy of the incident particle.

The two (p,n) reactions (Fig. 5) should be much simpler in their interpretation. The sharp peak at low energy would result from capture of the incident particle followed by the evaporation of a single neutron. This contribution becomes very small above ~30 Mev because of competition from the emission of several particles. Here the yield should be almost entirely from a single exchange collision in the nucleus with small momentum transfer. An analysis of the curves should give evidence as to whether the same ratio of ordinary to exchange forces as is required to explain free n-p

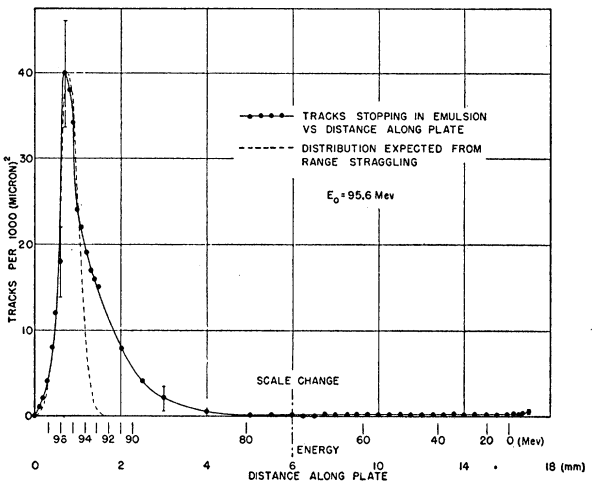

FIG. 7. Tracks stopping in NTA plate behind tapered absorber at 95.6 Mev.

[23] W. Heckrotte and P. Wolff, Phys. Rev. **73**, 264 (1948).
[24] G. F. Chew and M. L. Goldberger, Phys. Rev. **77**, 470 (1950); J. Hadley and H. York, Phys. Rev. **80**, 345 (1950).
[25] K. J. Le Couteur, Proc. Phys. Soc. (London) **A63**, 259 (1950).
[26] R. Serber, Phys. Rev. **72**, 1114 (1947).

scattering can be used to account for the p-n collisions between an incident particle and one in the nucleus.

The authors wish to thank Dr. Karl Strauch for his suggestion of the boron reaction and his help with this and other aspects of the experiment. Dr. Ralph Waniek and Dr. James Meadows have given considerable technical aid. Professor N. Bloembergen, Dr. P. J. van Heerden, and U. E. Kruse, were responsible for some very fruitful discussions. Arthur Hansen and Archie Grant were very helpful in the construction of apparatus and in the numerous cyclotron bombardments.

APPENDIX A

An estimate of the energy distribution of the "180°" scattered beam at the target position was obtained by exposing an Eastman NTA plate behind a tapered absorber.[27] The plate was then scanned along the direction of the taper, which was perpendicular to a cyclotron radius. The number of tracks which stopped in the emulsion, per unit length along the taper direction, was then proportional to the number of protons per unit range interval. The results are shown in Fig. 7 with standard deviations for typical points. The dotted line shows the distribution expected from range straggling alone if this distribution is normalized at the peak. The calculated broadening due to focusing error and width of plate scanned is negligible. The results seem to indicate the presence of a group of particles from 3–5 Mev less in energy and roughly 30 percent of the peak intensity. However, in order to limit the track density, even with $\frac{1}{10}$ sec exposure, it was necessary to detune the timing of the ion source pulsed high voltage to a point corresponding to a reduction by a factor of 30 in the normal beam, and to substitute helium for hydrogen as the ion source gas. This adjustment would drastically reduce the normal beam but have only a small effect on the spurious particles[28] which do not originate at the ion source. In addition, the peak of Fig. 7 was probably underestimated in relation to the rest of the curve since the high track density in that area would cause some tracks which stopped to be overlooked. The results here should be regarded as an upper limit to the energy width under normal operation conditions. The low energy protons may be the result of particles on a second or third traversal of the scatterer which penetrate beyond its innermost edge or to particles doubly scattered from the dee structure. A spread of as much as 2 or 3 Mev at 100 Mev would be easily seen in a discrepancy with the linear accelerator data[9] at the threshold. However, from this experiment it can be concluded that the values of the (p,n) cross sections at high energy cannot be in error by more than 10 percent because of the presence of low energy protons at the targets.

APPENDIX B

The loss of protons from the foil area of the absorber assembly by multiple Coulomb scattering has been mentioned as a source of error in the relative excitation functions. A brief summary is given here of an approximate calculation and an experiment bearing on this effect.

TABLE II. Results of calculation showing scattering losses $F(\tau)$, for various foil radii, r_f, and absorber radii, r_a.

Case	$\langle\Delta r^2\rangle_{Av}^{\frac{1}{2}}$ cm	r_f cm	r_a cm	$(r_a-r_f)/\langle\Delta r^2\rangle_{Av}^{\frac{1}{2}}$	$F(\tau)$ %
1. Brass	0.10	0.397	0.556	1.6	2
2. Brass	0.10	0.556	0.715	1.6	1.3
3. Brass	0.10	0.397	0.715	3.2	1
4. Aluminum	0.17	0.556	0.715	0.9	7.3
5. Aluminum	0.17	0.397	0.715	1.9	2.6

The multiple scattering theory of Williams[7] modified by Dickinson and Dodder[29] to include energy loss is used because of its analytical simplicity. The geometry of the target and absorber assembly is taken as a series of thin foils of radius, r_f, embedded coaxially in a solid cylinder of absorber of radius, r_a. It is assumed that only those protons are lost from the foil area whose displacements after penetrating a depth, τ, are such that they are found outside of the absorber area. Those protons which stray into the region between r_f and r_a are assumed to be approximately replaced by protons which are initially in this region and are scattered into the foil area.

Protons incident at a distance from the absorber center, r, will have, at a depth, τ, a displacement, Δr, projected along a radius. The distribution of Δr is Gaussian with the mean square displacement, $\langle\Delta r^2\rangle_{Av}$, given by[30] $\langle\Delta r^2\rangle_{Av}=\langle\alpha^2\rangle_{Av}\tau^2/3$, where $\langle\alpha^2\rangle_{Av}$ is the mean square projected scattering angle at a depth τ. $\langle\alpha^2\rangle_{Av}$ can be calculated from the formulas of Dickinson and Dodder. When the circular geometry is approximately taken into account, the fractional loss after a depth τ is

$$F(\tau)=\int_0^{\rho_f}\rho\rho_f^{-2}[1-\mathrm{erf}\rho_e]d\rho,$$

where $\rho_e=\frac{1}{2}[(2\rho_a-\rho^2)^{\frac{1}{2}}-\rho]$, the ρ's being the r's, defined above, in units of $\langle\Delta r^2\rangle_{Av}^{\frac{1}{2}}$. $F(\tau)$ was evaluated numerically for several values of r_f and r_a for brass and aluminum, each for an absorber thickness, τ, corresponding to an energy interval from 100 to 20 Mev. The results are shown in Table II.

This shows clearly the desirability of brass over aluminum absorbers and the critical dependence of F on the amount by which the absorber diameter exceeds the foil diameter (column 5). For most of the data presented here the geometry corresponds to case 3 for which the scattering loss is negligible. When aluminum absorbers were used to obtain small energy steps at low energy, a small discrepancy could be seen with the points taken with brass absorbers of the order of magnitude shown in Table II. This is shown in Fig. 2 where the final curve is drawn favoring the brass absorber points. An experiment to check the values calculated above was performed using $\frac{7}{16}$-in. foils in $\frac{9}{16}$-in. absorbers. After irradiation, the center $\frac{5}{16}$-in. diameter was punched out and the inner and outer areas counted separately. Since the scattering losses are almost entirely from the periphery of the foils, the ratio of the inner to outer area activities gives an estimate of $F(\tau)$. The result for a geometry resembling case 3 (brass absorbers) was $F\leq 1$ percent while for a geometry intermediate between cases 4 and 5 was $F=2\pm 1$ percent, in rough agreement with the calculated values.

[27] N. Bloembergen and P. J. van Heerden, Phys. Rev. **83**, 561 1951).

[28] Kruse, Mack, and Ramsey, Rev. Sci. Instr. **22**, 839 (1951).

[29] W. C. Dickinson and D. C. Dodder, Los Alamos Report No. 1182 (1950).

[30] B. Rossi and K. Greisen, Revs. Modern Phys. **13**, 240 (1941).